Supplementary Tables and Figures

Table S1. Details of small molecule candidates evaluated in this study

Well	Pubchem ID	Name
A1	NCGC00091250-04	Reserpine
B1	NCGC00168786-01	Deserpidine
C1	NCGC00167569-01	Mefeserpine
D1	NCGC00253604-01	Rescimetol
E1	NCGC00179331-02	NCGC00179331-01
F1	NCGC00017003-01	Prestwick-13C05
3TX8	NCGC00179590-02	Syrosingopine
A3	NCGC00016833-01	Halofantrine hydrochloride
B2	NCGC00015874-05	Quinacrine
C2	NCGC00165756-01	BiCAPPA
D2	NCGC00014300-01	500565-15-1
E2	NCGC00344515-03	Piperaquine
G2	NCGC00167490-01	Lumefantrine
3TX6	NCGC00263128-02	PD-0220245
B3	MLS003876812-01	Proflavine sulfate Hydrate
F2	NCGC00651732-01	ROC-325
H2	NCGC00110901-01	MLS000731354

Table S2. Plasma concentrations of Halofantrine

Animal ID	Tissue	Treatment	Timepoint	Volume (uL)	Conc (ng/mL)
33001	Plasma	25uM IVT	Baseline	100	BQL
33002	Plasma	25uM IVT	Baseline	100	BQL
33003	Plasma	25uM IVT	Baseline	100	BQL
33004	Plasma	25uM IVT	Baseline	100	BQL
33005	Plasma	25uM IVT	Baseline	100	BQL
33006	Plasma	25uM IVT	Baseline	100	BQL
33007	Plasma	25uM IVT	2h	250	BQL
33008	Plasma	25uM IVT	2h	250	BQL
33009	Plasma	25uM IVT	2h	250	BQL
33013	Plasma	25uM IVT	4h	250	BQL
33014	Plasma	25uM IVT	4h	250	BQL
33015	Plasma	25uM IVT	4h	250	BQL
33010	Plasma	25uM IVT	24h	250	BQL
33011	Plasma	25uM IVT	24h	250	BQL
33012	Plasma	25uM IVT	24h	250	BQL
33001	Plasma	25uM IVT	168h	250	BQL
33002	Plasma	25uM IVT	168h	250	BQL
33003	Plasma	25uM IVT	168h	250	BQL
33004	Plasma	25uM IVT	168h	250	BQL
33005	Plasma	25uM IVT	168h	250	BQL
33006	Plasma	25uM IVT	168h	250	BQL
33016	Plasma	25uM SCS	Baseline	100	BQL
33017	Plasma	25uM SCS	Baseline	100	BQL
33018	Plasma	25uM SCS	Baseline	100	BQL
33019	Plasma	25uM SCS	Baseline	100	BQL
33020	Plasma	25uM SCS	Baseline	100	BQL
33021	Plasma	25uM SCS	Baseline	100	BQL
33022	Plasma	25uM SCS	2h	250	BQL
33023	Plasma	25uM SCS	2h	250	BQL
33024	Plasma	25uM SCS	2h	250	BQL
33028	Plasma	25uM SCS	4h	250	BQL
33029	Plasma	25uM SCS	4h	250	BQL
33030	Plasma	25uM SCS	4h	250	BQL
33025	Plasma	25uM SCS	24h	250	BQL
33026	Plasma	25uM SCS	24h	250	BQL
33027	Plasma	25uM SCS	24h	250	BQL

33016	Plasma	25uM SCS	168h	250	BQL
33017	Plasma	25uM SCS	168h	250	BQL
33018	Plasma	25uM SCS	168h	250	BQL
33019	Plasma	25uM SCS	168h	250	BQL
33020	Plasma	25uM SCS	168h	250	BQL
33021	Plasma	25uM SCS	168h	250	BQL
33031	Plasma	25uM SubC	Baseline	100	BQL
33032	Plasma	25uM SubC	Baseline	100	BQL
33033	Plasma	25uM SubC	Baseline	100	BQL
33034	Plasma	25uM SubC	Baseline	100	BQL
33035	Plasma	25uM SubC	Baseline	100	BQL
33036	Plasma	25uM SubC	Baseline	100	BQL
33037	Plasma	25uM SubC	2h	250	BQL
33038	Plasma	25uM SubC	2h	250	BQL
33039	Plasma	25uM SubC	2h	250	BQL
33043	Plasma	25uM SubC	4h	250	BQL
33044	Plasma	25uM SubC	4h	250	BQL
33045	Plasma	25uM SubC	4h	250	BQL
33040	Plasma	25uM SubC	24h	250	BQL
33041	Plasma	25uM SubC	24h	250	BQL
33042	Plasma	25uM SubC	24h	250	BQL
33031	Plasma	25uM SubC	168h	250	BQL
33032	Plasma	25uM SubC	168h	250	BQL
33033	Plasma	25uM SubC	168h	250	BQL
33034	Plasma	25uM SubC	168h	250	BQL
33035	Plasma	25uM SubC	168h	250	BQL
33036	Plasma	25uM SubC	168h	250	BQL

Supplemental Figures

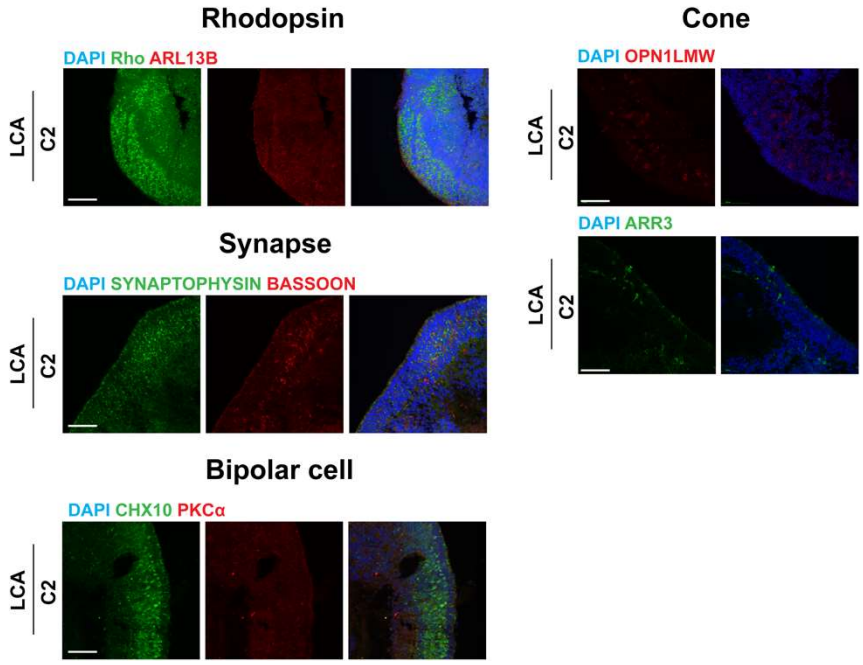

Figure S1. Various cell types in *CEP290*-LCA retinal organoids treated with compound C2

Immunostaining of various cell types including rod (Rhodopsin, green), cilia (ARL13B, red), ribbon synapses (BASSOON, red), presynaptic vesicles (SYNAPTOPHYSIN, green), bipolar cells (CHX10, green; PKCα, red), L/M cones (OPN1LMW, red), cone photoreceptors (ARR3, green). Nuclei were stained with 4',6-diamidino-2-phenylindole (DAPI). Images are representative of at least three independent experiments, each of which had at least four organoids. The scale bar represents 50 μm.

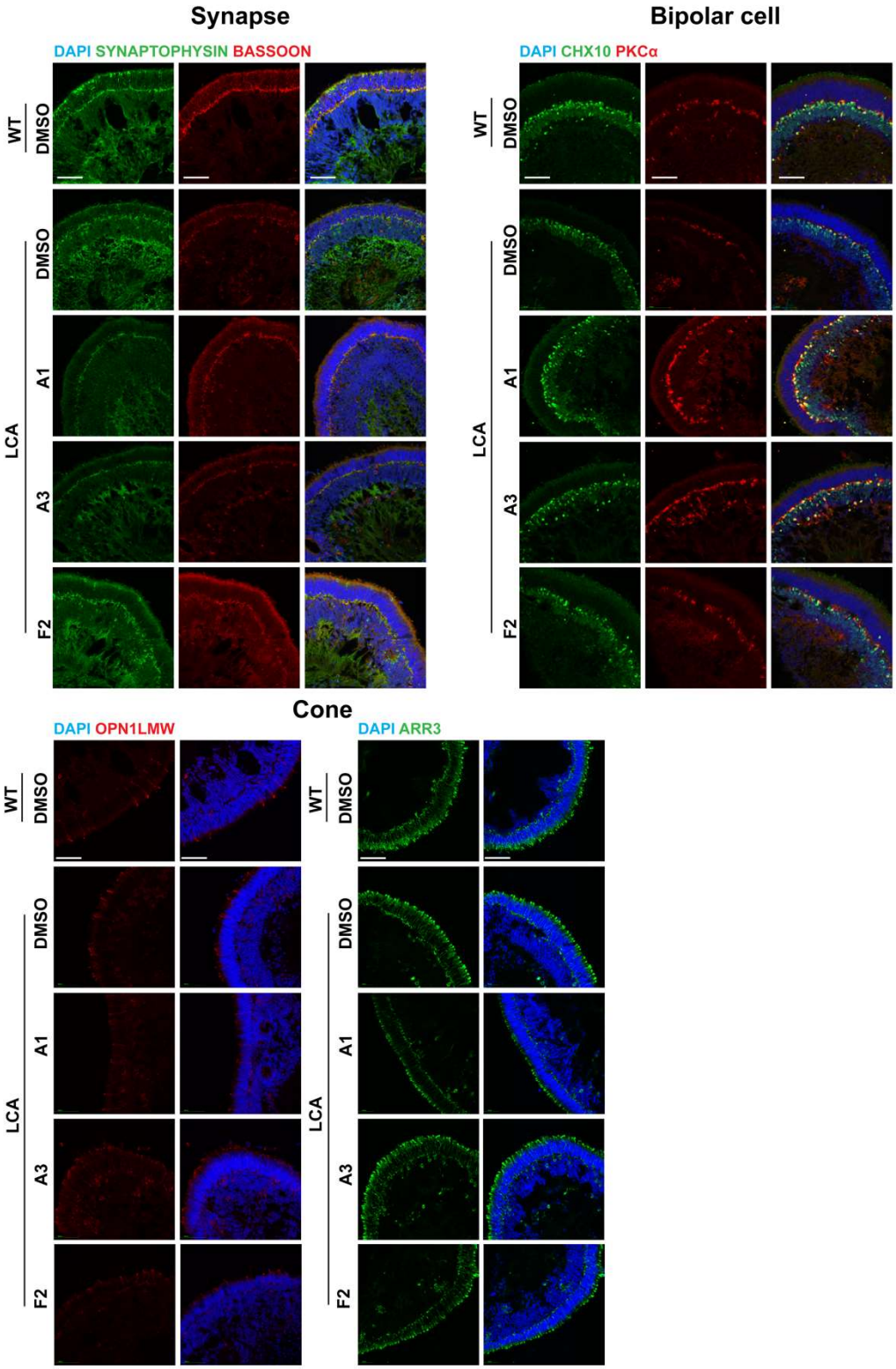

Figure S2. Various cell types in WT and *CEP290*-LCA retinal organoids treated with individual compounds

Immunostaining of structural or cell type-specific markers including ribbon synapses (BASSOON, red), presynaptic vesicles (SYNAPTOPHYSIN, green), bipolar cells (CHX10, green; PKCα, red), L/M cones (OPN1LMW, red), cone photoreceptors (ARR3, green). Nuclei were stained with 4',6-diamidino-2-phenylindole (DAPI). Images are representative of at least three independent experiments, each of which had at least four organoids. The scale bar represents 50 μm.

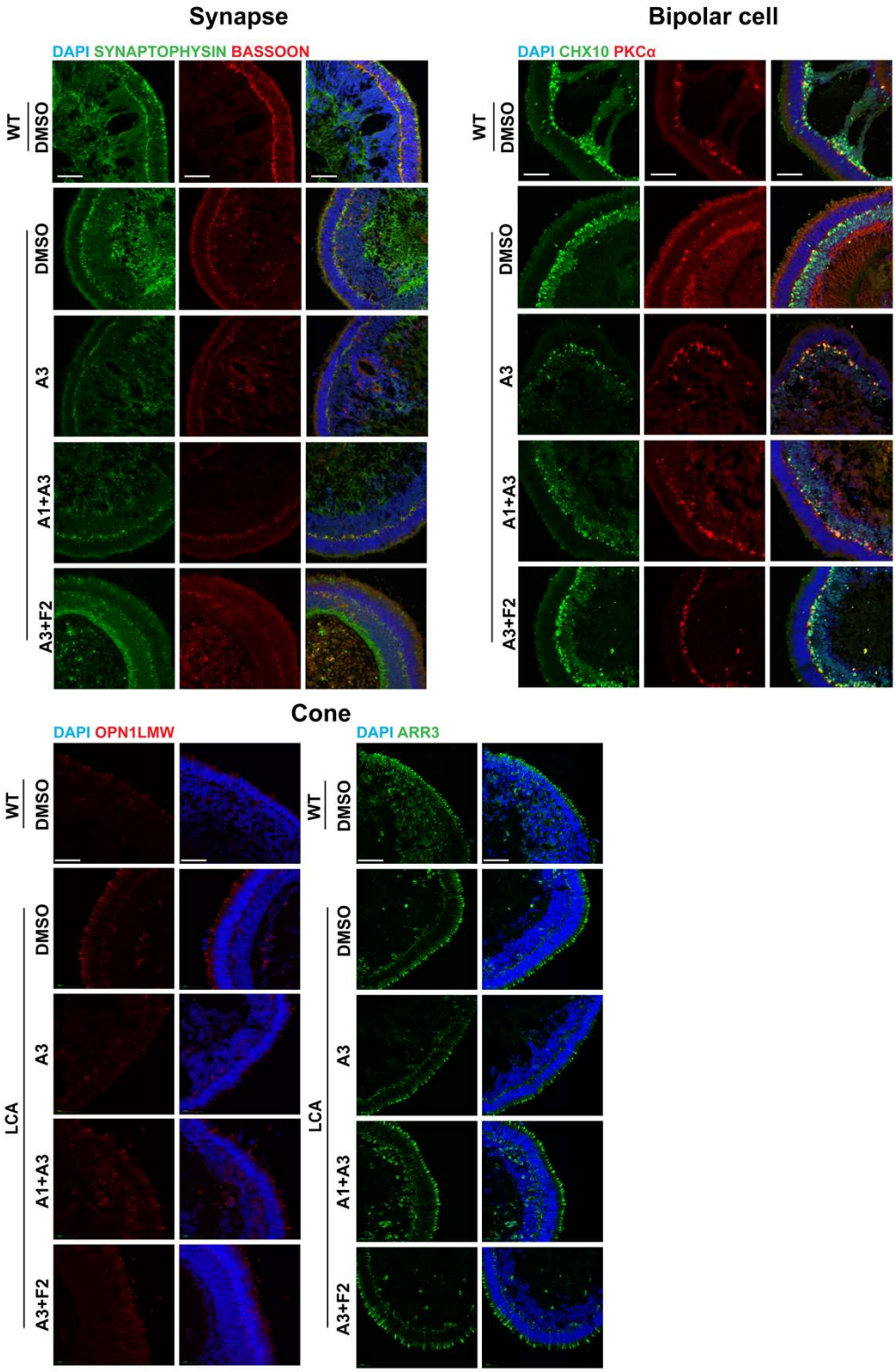

Figure S3. Various cell types in WT and *CEP290*-LCA retinal organoids treated with compound A3 and combinations with other compounds

Immunostaining of structural or cell type-specific markers including ribbon synapses (BASSOON, red), presynaptic vesicles (SYNAPTOPHYSIN, green), bipolar cells (CHX10, green; PKCα, red), L/M cones (OPN1LMW, red), cone photoreceptors (ARR3, green). Nuclei were stained with 4',6-diamidino-2-phenylindole (DAPI). Images are representative of at least three independent experiments, each of which had at least four organoids. The scale bar represents 50 μm.

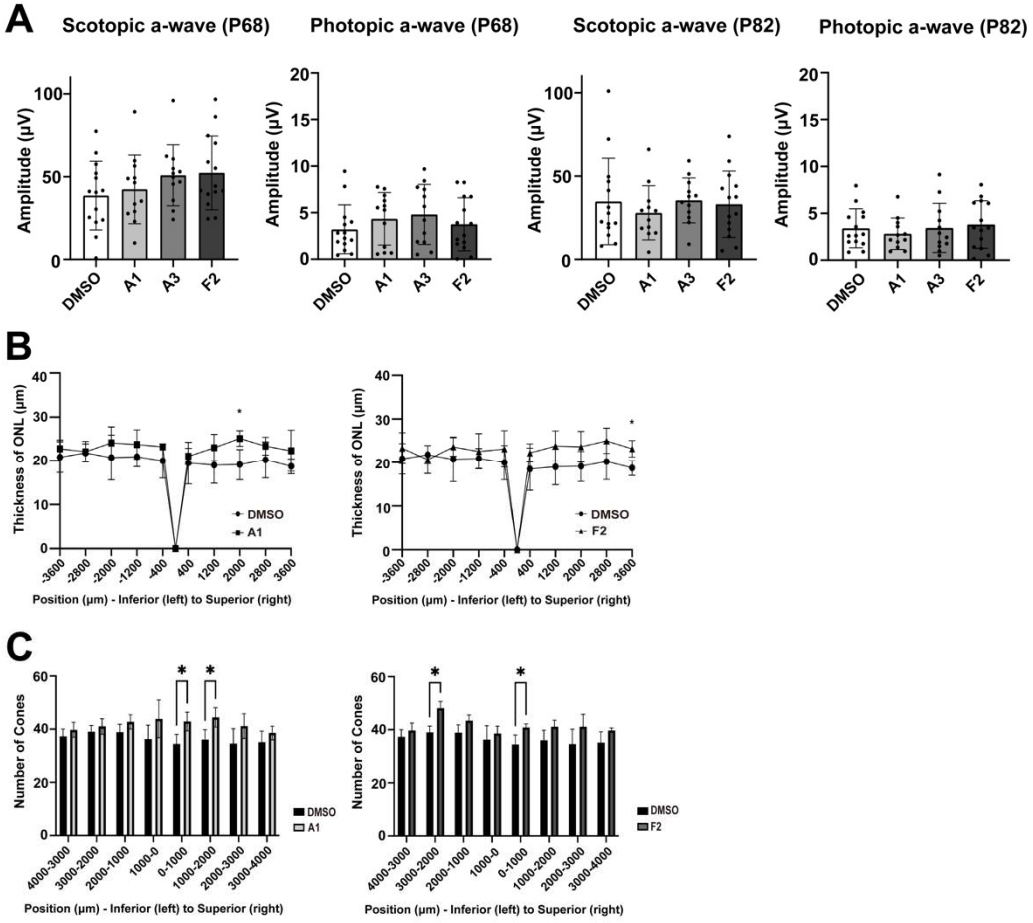

Figure S4. Functional and structural evaluation of potent candidates in P23H rats
(A) Scotopic and photopic b-wave ERG responses at P68 and P82 in DMSO- and compound-treated P23H rats. Data are presented as mean ± SEM, and the Brown-Forsythe and Welch ANOVA tests were used to compare 7 DMSO- and 6 or 7 compound-treated rats. **(B)** Analysis of ONL thickness using DAPI-stained retinal sections at P84. **(C)** The numbers of cone photoreceptors was counted every 1000 µm throughout the retina. Data are presented as mean ± SEM, using Mann-Whitney U test. *P < 0.05

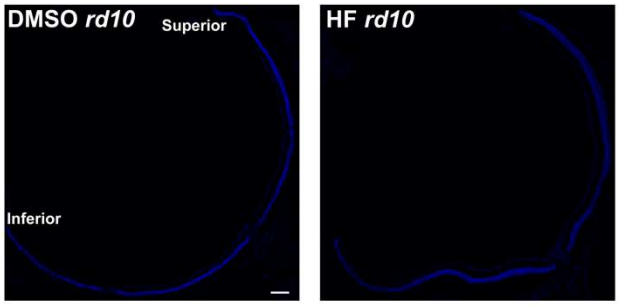

Figure S5. Representative images of whole retinal sections from DMSO- and Halofantrine (HF)-treated *rd10* mice

Representative whole-retina sections stained with DAPI at P36. The scale bar represents 100 μm. HF, Halofantrine.

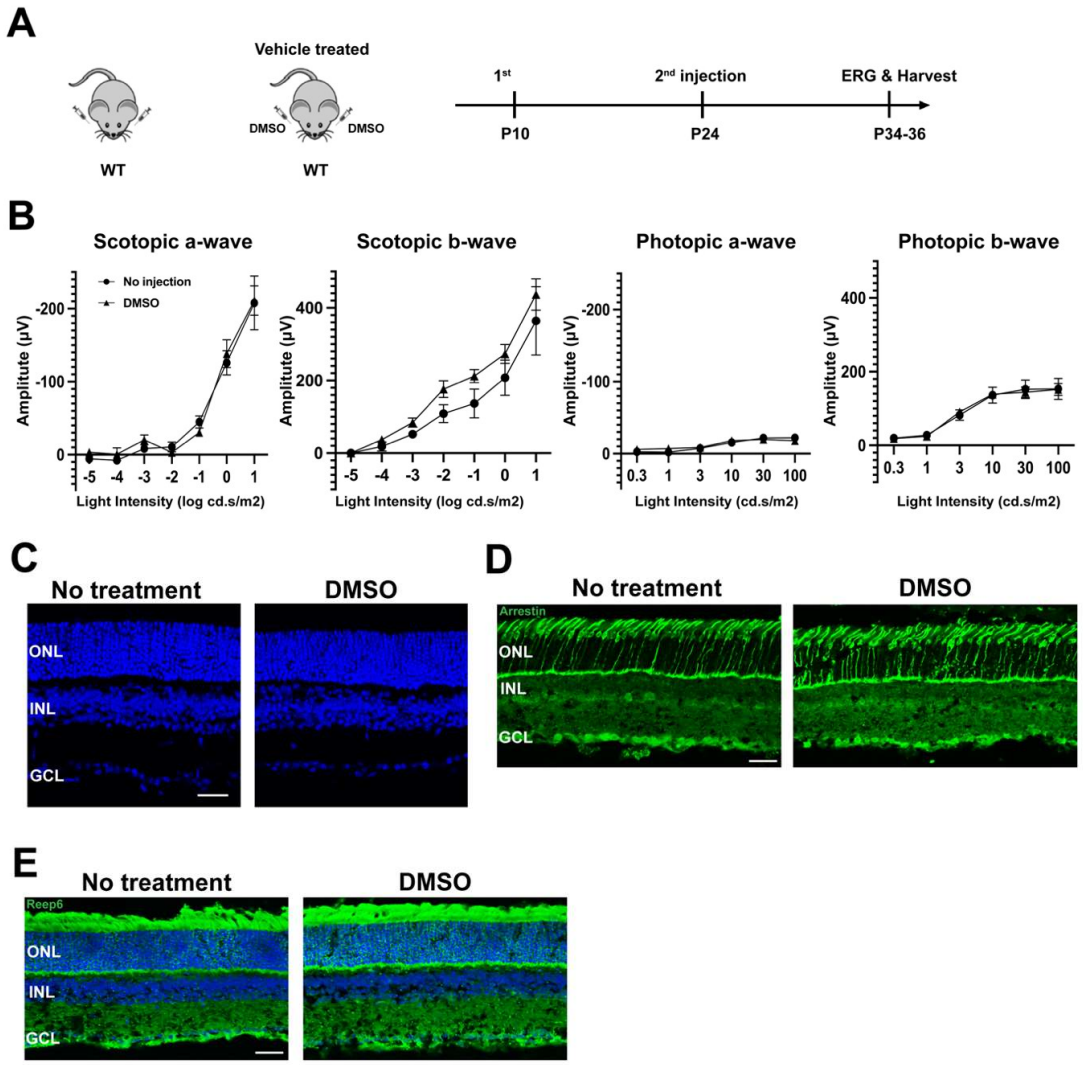

Figure S6. Effect of DMSO in WT mice

(A) Timeline of in vivo intravitreal injections for quantification of outer nuclear layer thickness (ONL), retinal morphology, and immunohistochemistry studies. **(B)** Scotopic and photopic electroretinogram responses in untreated and DMSO-treated WT mice. **(C)** Outer nuclear layer thickness evaluated in DAPI-stained retinal sections at P36. The representative images were taken from the superior retina, 1800 μm away from the optic nerve. Data are presented as mean ± SEM, and the Mann-Whitney U test was used to compare untreated and DMSO-treated groups. Images are representative of eight mice. **(D)** Cone photoreceptors were evaluated by immunostaining of cone arrestin at P36. The number of cone photoreceptors was counted every 500 μm throughout the retina. Data are presented as mean ± SEM, and the Mann-Whitney U test was used to compare untreated and DMSO-treated groups. **(E)** Rod photoreceptors were evaluated by immunostaining for REEP6 (green) at P36. Representative images were obtained from retinal regions where the most significant changes were observed. The scale bar represents 20 μm.

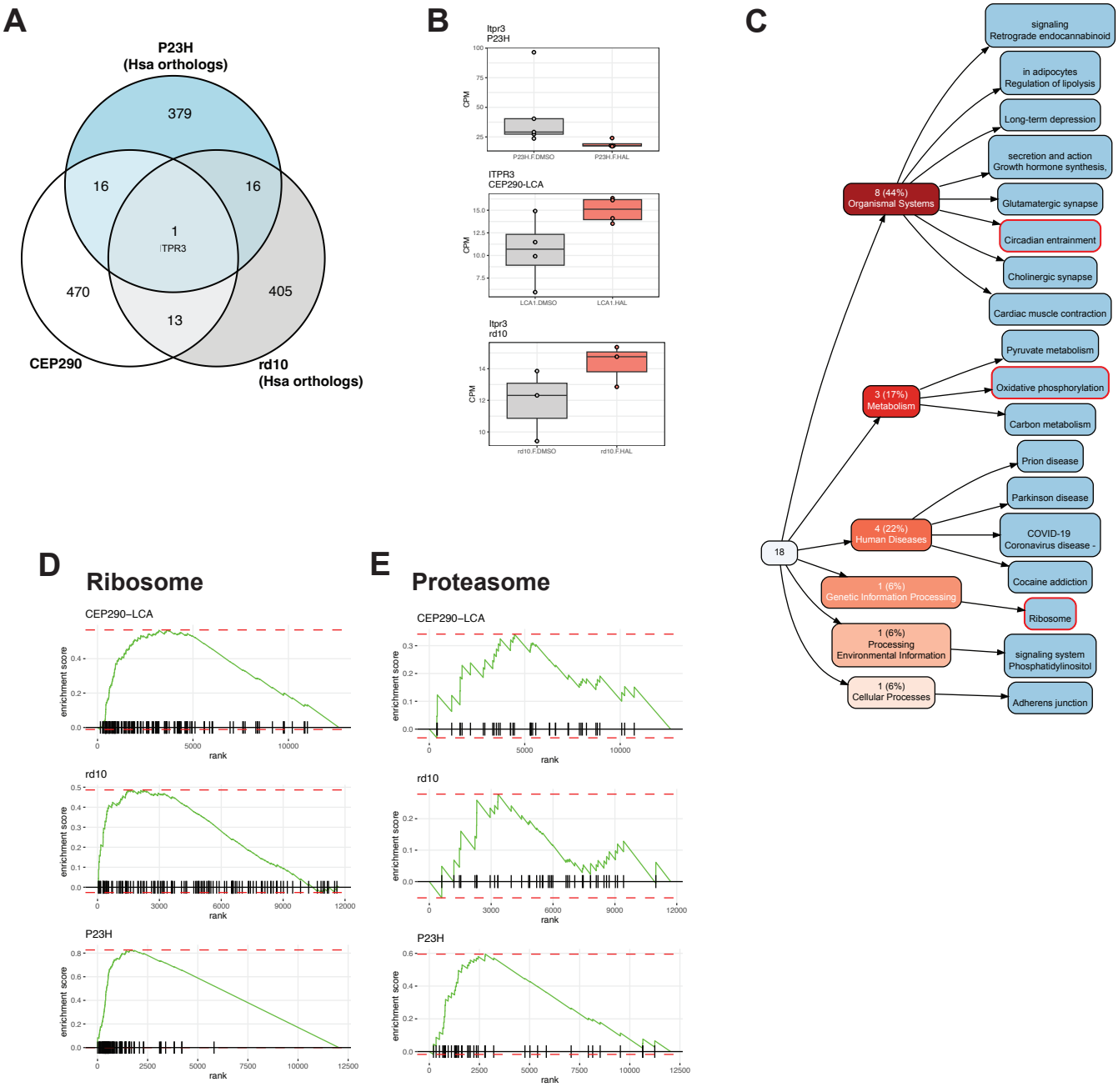

Figure S7. Functional analysis of halofantrine treatment in retinal disease models.
(A) Venn diagram showing intersections in halofantrine linked DEGs in the various IRD models. P23H and rd10 DEGs were converted to corresponding human aliases for comparison. **(B)** Boxplot of Itpr3 expression in treated and untreated IRD models. **(C)** List of halofantrine responding KEGG pathways shared between two or more disease models. **(D,E)** Enrichment plot of Ribosome and Proteasome genesets after drug treatment.

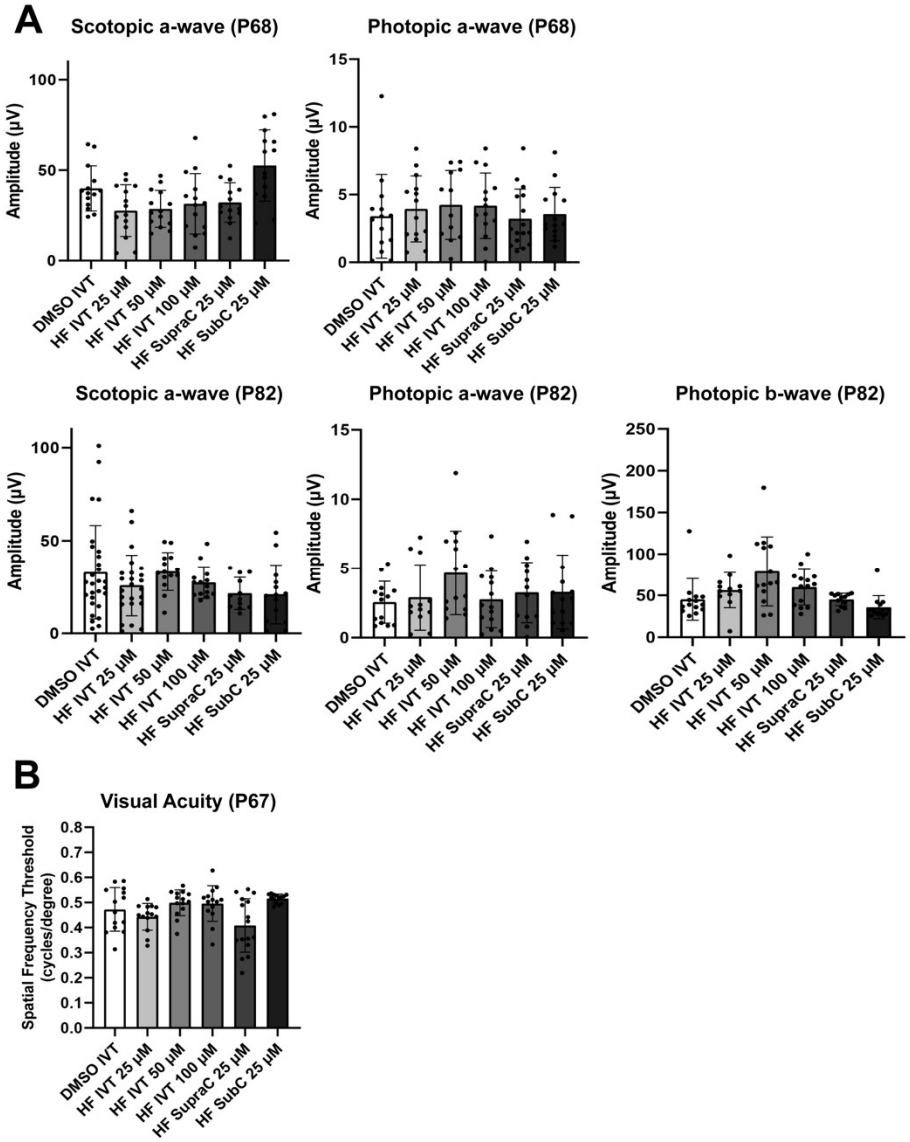

Figure S8. ERG and OKT responses in halofantrine-treated P23H rats
(A,B) Functional ERG and OKT outcomes following halofantrine administration via various ocular routes and dosages in P23H rats (n=7 per group). Data are presented as mean ± SEM, and the Brown-Forsythe and Welch ANOVA tests were used to compare the groups.

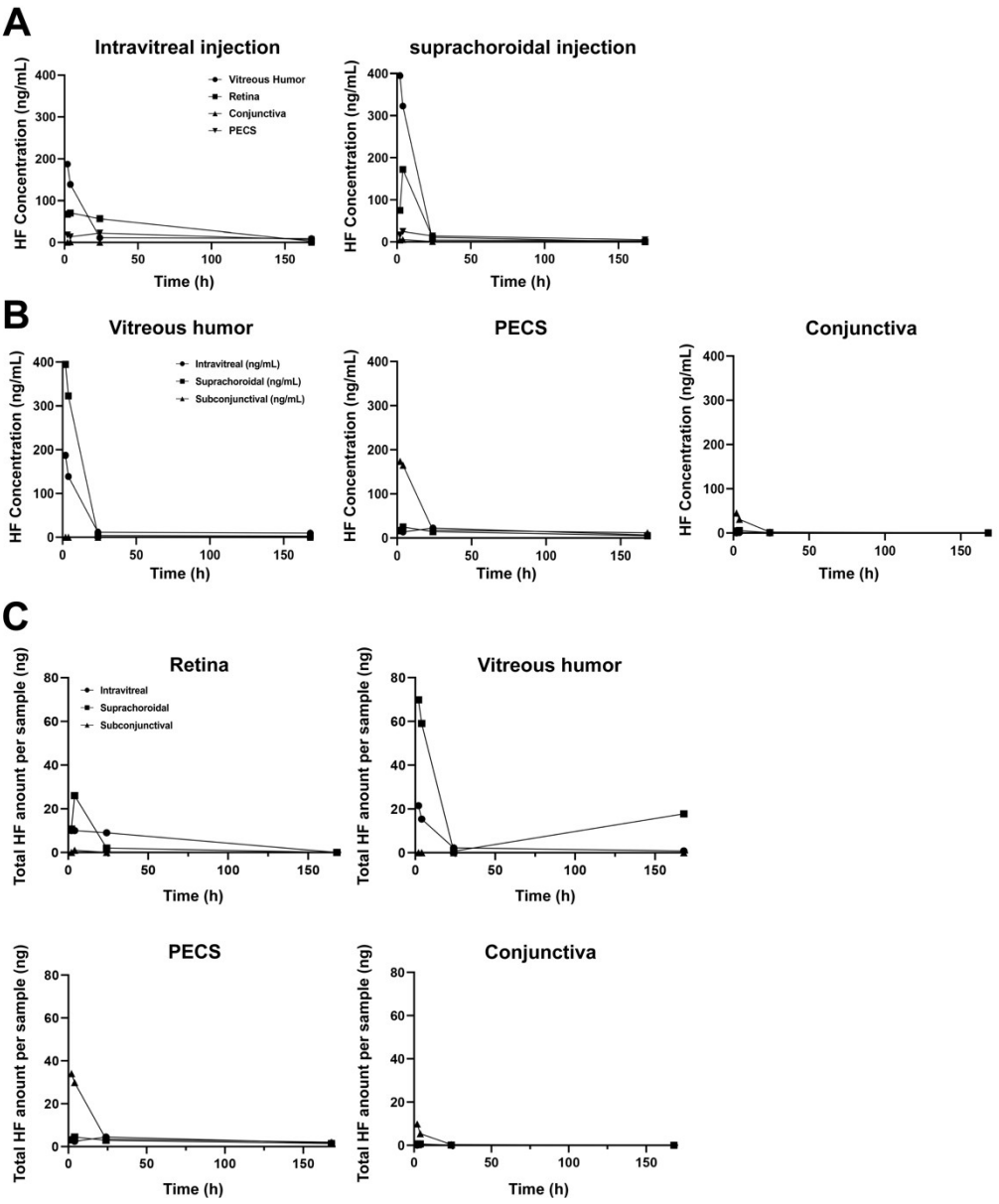

Figure S9. Ocular pharmacokinetics and tissue distribution of halofantrine
(A) Comparison of halofantrine distribution across various ocular tissues following intravitreal and suprachoroidal administration. **(B)** Pharmacokinetics and ocular tissue distribution of halofantrine following different delivery routes in WT rats. **(C)** Absolute amounts of halofantrine (ng) detected in individual ocular tissues after administration via three different injection routes (62.5 ng per eye).